Available online at www.sciencedirect.com
ScienceDirect
Surface & Coatings Technology 201 (2007) 8939–8943
SURFACE & COATINGS TECHNOLOGY
www.elsevier.com/locate/surfcoat

A novel CVD/CVI reactor with an in-situ sampling apparatus connected to an online GC/MS

Aijun Li, Günter Schoch, Sven Lichtenberg, Dan Zhang, Olaf Deutschmann *

Institut für Technische Chemie und Polymechemie, Universität Karlsruhe, 76131 Karlsruhe, Germany

Available online 22 May 2007

Abstract

Spatially resolved analysis of the composition of the gas-phase during chemical vapor deposition depends on an effective sampling apparatus. In the present work, a novel in-situ sampling and cooling apparatus was presented, which is connected directly to an online GC/MS. Simulations of the temperature distribution in the cooling apparatus show that sample gas can be cooled down to 600 K in short time, resulting in a gas-phase composition quench. This device was employed to analyze gas-phase composition resulting from the pyrolysis of methane. Experiments were carried out at an oven temperature of 1150 °C to investigate the composition along the axis of a tubular reactor. Flow fields of the tubular reactor were predicted numerically neglecting volume changes due to chemical reactions involved in methane decomposition.

Keywords: Chemical vapor deposition; Pyrolytic carbon; Decomposition; Simulation

1. Introduction

Chemical vapor deposition/infiltration (CVD/CVI) of pyrolytic carbon is one of the most attractive methods for the production of high-quality carbon/carbon (C/C) composites frequently used in high-temperature applications, such as rocket nozzles, airplane brakes, and furnace components [1–3]. CVD/CVI processes make it possible to obtain C/C composites with excellent mechanical and thermal properties; therefore many studies have been devoted to a better understanding of this process in order to obtain better control and higher production efficiency of C/C composites in the past several decades [4,5]. One of the hot issues related to CVD/CVI of C/C composites is to analyze gas-phase composition and then try to correlate it with microstructures of pyrolytic carbon deposited on planar surfaces (in CVD) or inner surfaces of porous fiber preforms (in CVI) [6–12].

However, accurate analysis of gas-phase composition depends on an effective sampling apparatus. Tubular reactors are popular for CVD of hydrocarbons. Usually, the GC/MS is connected to the outlet of tubular reactors to analyze the composition of the gas-phase; however it is obvious that the measured composition is not the in-situ gas-phase composition of CVD. Thus a quench system is necessary to investigate the variation of the composition of the gas phase along the axis of the tubular reactor.

Gas-phase composition of methane pyrolysis has widely been investigated with static systems in CVD of carbon or in the studies of the conversion of natural gas into higher molecular weight fuels [13,14]. In the present work, an in-situ sampling apparatus for the gas-phase composition was added to a tubular flow reactor and effective cooling of the sampled gas was implemented to analyze the composition of the gas-phase resulting from the pyrolysis of methane. Moreover, simulation of flow fields is also performed.

2. Experimental

2.1. Set-up of the tubular reactor

The tubular reactor used in the present work is shown in Fig. 1 (a). Fig. 1 (b) shows the in-situ sampling apparatus made of quartz glass and Fig. 1 (c) shows the detail of the cooling part (for composition quenching). The vacuum of cooling part can be kept as low as around 700 Pa, considerably reducing heat transfer from the oven to the cooling gas. The diameter of the hole of the in-situ sampling device is 1 mm; flow rate of the

* Corresponding author. Tel.: +49 721 608 3138; fax: +49 721 608 4805.
E-mail addresses: li@ict.uni-karlsruhe.de (A. Li), deutschmann@ict.uni-karlsruhe.de (O. Deutschmann).

0257-8972/$ - see front matter © 2007 Elsevier B.V. All rights reserved.
doi:10.1016/j.surfcoat.2007.05.010

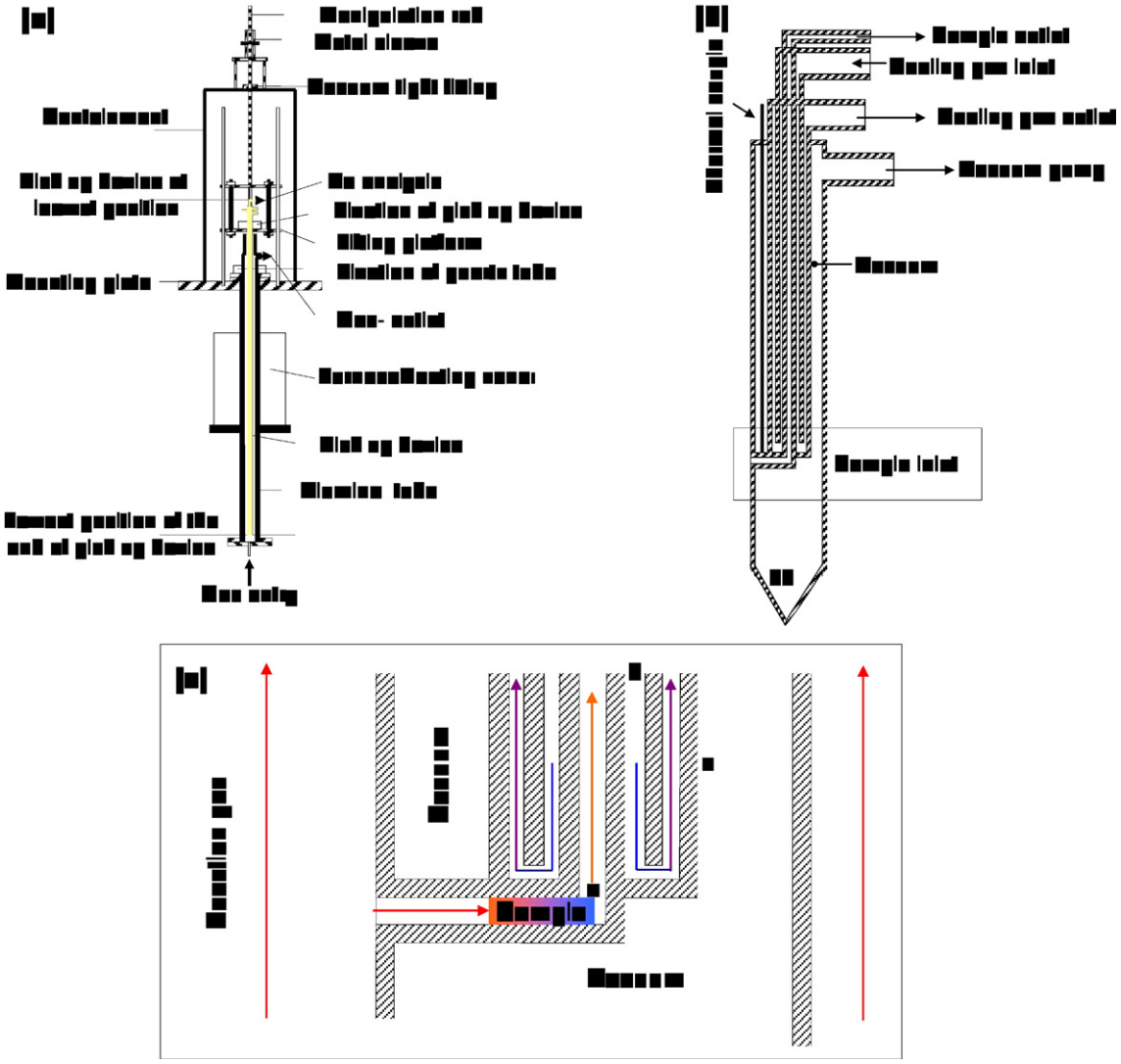

Fig. 1. Schematic illustration (not to scale) of the tubular reactor (a), the in-situ sampling and composition quench apparatus (b), and local view (c).

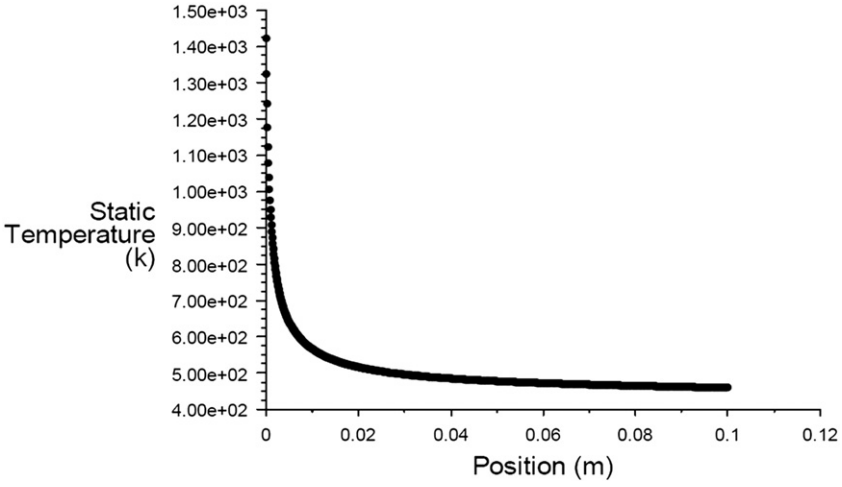

Fig. 2. Simulation results of temperature distribution of the cooling part.

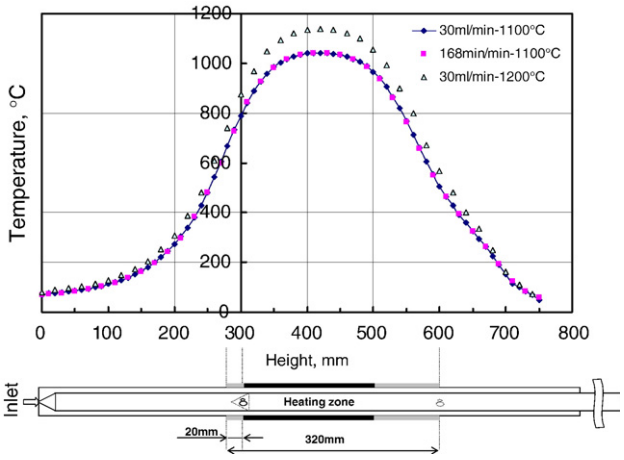

Fig. 3. Temperature profiles of the reactor measured for the empty tube.

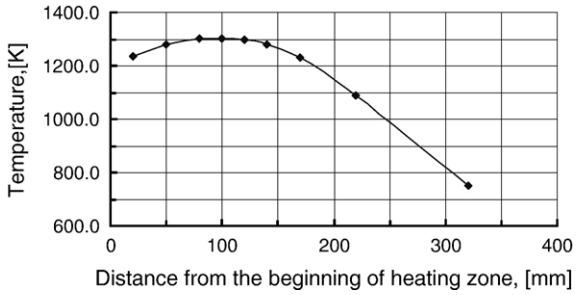

Fig. 4. Temperature distribution in the tubular reactor measured using the thermal couple of the in-situ sampling device.

cooling gas (Argon) is about 2.5 l/min. The temperature of the sample gas was measured using a thermal couple fixed close-by the sampling hole (shown in Fig. 1b). The in-situ sampling device is connected to a HP GC/MS calibrated for methane, acetylene, ethylene, propine, benzene and toluene.

Simulation of the temperature profile of the cooling part was carried out using the software "Fluent6.1.22" (Linux version). The corresponding boundary conditions are: temperatures at sample gas inlet ("a", as shown in Fig. 1c) and at external surface of the cooling part ("c") are assumed to be 1273 K and 473 K, respectively; the velocities at the sample gas inlet and at the cooling gas inlet ("b") are 1.18 m/s and 3.32 m/s, respectively. Fig. 2 shows the simulation results. It seems that the

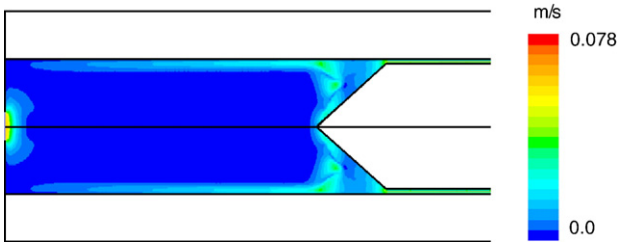

Fig. 5. Simulated flow field from the bottom of the reactor to the in-situ sampling apparatus (Flow rate at the inlet: 0.059 m/s).

Table 1
Typical example of the original FID data for the composition of a gas phase picked up by the in-situ sampling device and analyzed by MSD chemStation (distance from the beginning of heating zone is 200 mm)

Signal: 1210LI-10CH490AR-200-1.D\FID2 B.CH

Peak #	Ret time	Type	Width	Area	Start time	End time	Species	Partial pressure (kPa)
1	2.760	BV	0.033	137,120,343	2.701	2.951	CH_4	8.025180826
2	3.976	BV	0.037	2,985,588	3.871	4.011	C_2H_2	0.159367073
3	4.041	VB	0.040	2,162,178	4.011	4.175	C_2H_4	0.09484012
4	8.129	VB	0.037	600,311	8.086	8.263	P-C_3H_4	0.017935875
5	13.680	BB	0.043	3,853,643	13.430	13.796	C_6H_6	0.211567884
6	15.078	BB	0.035	343,450	15.023	15.216	C_7H_8	0.045234153
7	17.355	BB	0.129	4,466,443	17.150	17.710	$C_{10}H_8$	No calibration data

sample gas can be cooled down to 600 K within approximately 0.008 s, avoiding further pyrolysis of hydrocarbons. Fig. 3 shows the temperature profiles for two oven temperatures as well as for two flow rates of Argon; this measurement was performed using the empty tubular flow reactor. The distance from the lowest position to the highest position at which gas composition can be measured is 320 mm, thus the entire length of the heating zone can be covered. In the present work, the temperature of the oven is set to 1423 K and the temperature profile of heating zone measured by the thermal couple of the in-situ sampling device is shown in Fig. 4.

The total pressure in the tubular reactor is 100 kPa and partial pressure of methane is 10 kPa. Argon is also used as the diluted gas of the reactor. At the inlet the total volume flow of the gas mixture is 100 ml/min, leading to an average gas velocity of 0.059 m/s (corresponding to an inlet diameter of 6 mm). Simulation of velocity distribution of the reactor was also performed, using Fluent6.1.22. Non-isothermal flow was simulated at boundary conditions of constant heat transfer coefficients and the heating zone temperature of 1273 K. Fig. 5 shows the calculated flow field at the condition of pure argon, corresponding to the gas-pick-up hole positioned at the middle of the heating zone. Some recirculation loops seem to be present close to the sampling apparatus cone; those loops, however, are situated in a low temperature zone (as shown in Fig. 3) and therefore will not result in substantially adverse effect on the control of residence time from the view point of methane pyrolysis.

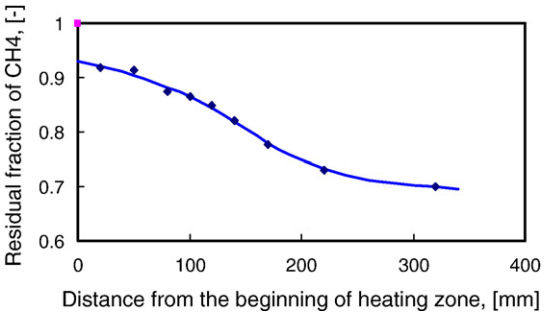

Fig. 6. Residual fraction of methane as a function of the distance from the beginning of the heating zone (error limit: ±0.19%).

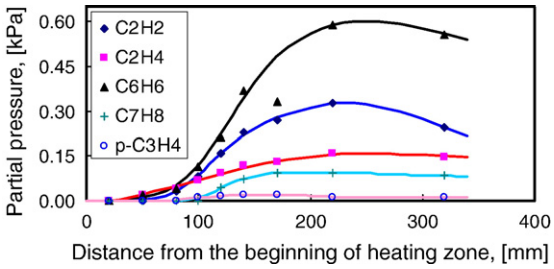

Fig. 7. Partial pressures of intermediate species in methane pyrolysis (error limits, C_2H_2:−4.1%, C_2H_4:−2.4%, C_6H_6: 10.8%, C_7H_8: 12.2% and p-C_3H_4: −11.5%).

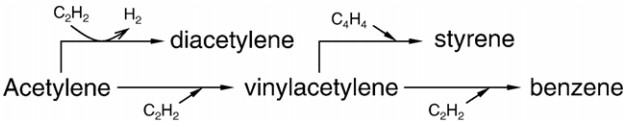

Fig. 8. The sketch of reaction flow in acetylene pyrolysis.

2.2. Result and discussion

In Table 1 an example of the data following from a chromatogram of the gas phase picked up by the in-situ sampling device, recorded by FID and evaluated by MSD chemStation is compiled. With the calibration data of GC/MS, partial pressures of gas-phase species were obtained. Fig. 6 shows the residual fraction of methane as a function of the distance from the beginning of the heating zone z. Extrapolation of the experimental data z=0 shows that the pre-decomposition of methane is about 7%. As shown in Fig. 4, the temperature reaches around 900 °C before gas mixture enters the heating zone (at z=0). At a temperature of 900 °C and a short residence time, pyrolysis of methane can be neglected. This implies that the pre-decomposition of methane should results from a still lower flow rate of cooling gas in the in-situ sampling device.

Former studies of methane pyrolysis showed the partial pressure of benzene is always lower than that of acetylene [15]. In the present work, however, the measured partial pressure of benzene is higher than that of acetylene, as illustrated in Fig. 7. Hüttinger and coworkers believed that C_4 species is the most likely intermediary in the formation of benzene in methane pyrolysis while C_3 species should only be of minor importance. Moreover, they never detected any C_3 species. Based on experimental studies of carbon deposition from ethylene, acetylene and propylene, Norinaga and Deutschmann proposed a detailed elementary reaction mechanism (consisting of 827 reactions among 227 species) giving a deeper insight into homogeneous gas-phase reactions [16–18]. Their reaction flow analysis of acetylene shows the addition of vinylacetylene on acetylene is the key pathway for the formation of benzene as summarized in Fig. 8. Their calculations also show C_3 species plays the same role with C_4 species on formation of aromatic species though 1,3-butadiene becomes the most important intermediary due to an increased content of vinyl in the gas-phase composition of ethylene pyrolysis as summarized in Fig. 9. As the reaction flow analysis of the pyrolysis of propylene shows C_3 species have crucial effect on formation of benzene as summarized illustrated in Fig. 10.

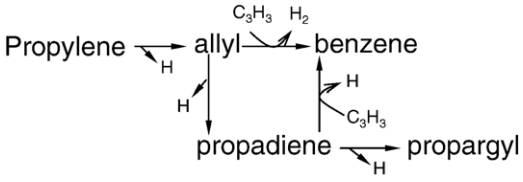

Fig. 10. The sketch of reaction flow in propylene pyrolysis.

In the work of Ziegler and coworkers, a detailed kinetic mechanism (87 species involved in 386 reactions) was proposed for the pyrolysis of propane [7–9]. Flux analysis (T=1248 K, residence time=1 s) shows C_3 species exist as a very important intermediary forming three ‘‘families’’ of products, namely the ‘‘C_4’’, benzene and the products derived from it, and those of cyclopentadiene, while the ‘‘C_4’’ has no direct contribution to the formation of aromatic species. They also pointed out the possibility of the transformation of ‘‘five-membered ring’’ into ‘‘six-membered ring’’ resulting from the formation of resonant structures by abstraction of a hydrogen atom, bonded to the methyl group.

All those former studies show that the pathway for formation of aromatic species depends on the presence of stabilized free radicals with high concentrations such as propargyl, allyl and cyclopentadienyl in gas-phase composition. Except for acetylene pyrolysis, proparagyl plays the leading role in the evolvement of gas-phase compositions.

Methane is a relatively stable species under conditions of the present work. There is no doubt that the initiating step of methane pyrolysis forms the methyl radical and that the hydrogen radical strongly accelerates the reaction. But it is still disputed for the formation of ethane and ethyl from methane, e.g. by reactions (1) and (2) shown in Table 2.

In most studies of combustion, eqn (2) is seldom mentioned. Preliminary calculations based on Norinaga’s mechanism show that this reaction has to be included in the mechanism to reproduce the experimental profile of methane. With one accord, ethane is

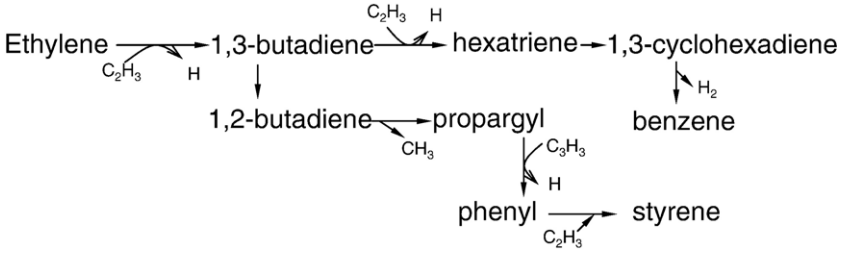

Fig. 9. The sketch of reaction flow in ethylene pyrolysis.

Table 2
List of elementary reactions mentioned in the text

No.	Reaction	$k=AT^n exp(-E/RT)$		
		A ($m^3\ s^{-1} mol^{-1}$)	n	E (kJ mol^{-1})
1	$CH_4+CH_3=C_2H_6+H$	8.000E+13	0.0	167.37
2	$CH_4+CH_3=C_2H_5+H_2$	1.000E+13	0,0	96.24
3	$C_2H_2+CH_3=p\text{-}C_3H_4+H$	1.000E+13	−0.53	56.07
4	$C_2H_2+CH_3=\alpha C_3H_5$	1.400E+04	2.21	69.04
5	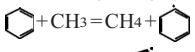	2.000E+12	0,0	62.7
6	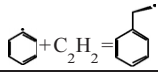	9.900E+41	−9.26	65.69

hardly detected while ethylene is formed very early in our experiments. Formation of acetylene follows by dehydrogenation of ethylene. Because of existence of high amount of methyl, ethylene and acetylene are dramatically consumed, leading to formation C_3 species as shown in reactions (3) and (4) of Table 2.

After then, methane pyrolysis shows similar evolving tendency with pyrolysis of propane: benzene is formed directly from propargyl; five-membered ring species are formed by addition of C_3 species on ethylene or acetylene; transformation of "five-membered ring" into "six-membered ring" results in increasing amount of aromatic species. Growth of polycyclic aromatic hydrocarbons [19] (PAH) should then follow in the gas-phase composition, but how does it work? Preliminary calculations based on Norinaga's mechanism also show high concentration of methyl, which will results in relatively higher concentration of light aromatic radicals (reaction (5) of Table 2.). Then addition of free radical on acetylene follows by a stabilization (reaction (6) of Table 2.)

For simulation, kinetic data of H-abstraction from PAH can be deduced by the similarity between structure and reactivity, though very few kinetic data are available from PAH larger than benzene or toluene. Hydrogen abstraction acetylene addition mechanisms of PAH Formation [19](HACA mechanism) will be activated if growth of aromatic species follows reactions (5) and (6), which would consume more C_2H_2 for the formation of PAHs, while affecting C_6H_6 in fewer amounts. That is the possible explanation for the surprising C6H6/C2H2 ratio we observed as shown in Fig. 7.

3. Conclusions

An in-situ sampling and composition quench apparatus was introduced into a typical tubular CVD/CVI reactor to analyze gas-phase variation along the axis of the reactor. Gas-phase composition of methane pyrolysis was measured by a DC/MS connected to this special in-situ sampling device. Comparison between simulation and experimental results imply pre-decomposition results from lower flow rate of cooling gas of the in-situ sampling device. A surprisingly high C_6H_6/C_2H_2 ratio was observed. Higher concentration of methyl leads to enough sources of aromatic radicals, which probably activate HACA mechanism playing key role in the consumption of acetylene.

Acknowledgment

This research was performed in the Sonderforschungsbereich 551 "Carbon from the gas phase: elementary reactions, structures, materials". Financial support by the Deutsche Forschungsgemeinschaft is gratefully acknowledged.

References

[1] T.M. Besmann, B.W. Sheldon, R.A. Lowden, D.P. Stinton, Science 253 (1991) 1104.
[2] E. Fitzer, L.M. Manocha, Carbon Reinforcements and Carbon/Carbon Composites, Springer, Berlin, Heidelberg, 1998, p. 190.
[3] G. Savage, Carbon–Carbon Composites Chapman & Hall, London, 1992.
[4] K.J. Hüttinger, Adv. Mater.-CVD 4 (4) (1998) 151.
[5] P. Delhaès, Carbon 40 (2002) 641.
[6] H.J. Li, A.J. Li, R.C. Bai, K.Z. Li, Carbon 43 (2005) 2937.
[7] I. Ziegler-Devin, R. Fournet, P. Marquaire, J. Anal. Appl. Pyrolysis 79 (1–2) (2007) 268.
[8] I. Ziegler, R. Fournet, P. Marquaire, J. Anal. Appl. Pyrolysis 73 (2) (2005) 231.
[9] I. Ziegler, R. Fournet, P. Marquaire, J. Anal. Appl. Pyrolysis 73 (2) (2005) 212.
[10] G.L. Vignoles, F. Langlais, C. Descamps, A. Mouchon, H. Le Poche, N. Reuge, N. Bertrand, Surf. Coat. Technol. 188–189 (2004) 241.
[11] J. Lavenac, F. Langlais, O. Féron, R. Naslain, Compos. Sci. Technol. 61 (3) (2001) 339.
[12] H.O. Pierson, M.L. Lieberman, Carbon 13 (1975) 159.
[13] R.F. James, P.A. Raymond, A.H. Timothy, A.D. Brent, Ind. Eng. Chem. Res. 41 (2002) 1425.
[14] A.M. Dean, J. Phys. Chem. 94 (1990) 1432.
[15] A. Becker, K.J. Hüttinger, Carbon 36 (3) (1998) 213.
[16] K. Norinaga, O. Deutschmann, K.J. Hüttinger, Carbon 44 (9) (2006) 1790.
[17] K. Norinaga, O. Deutschmann, Proc. of 15th European Conference on Chemical Vapor Deposition, Electrochem. Soc. Proc., vol. 9, 2005, p. 348.
[18] O., Deutschmann, S., Tischer, C., Correa, D., Chatterjee, S., Kleditzsch, V.M., Janardhanan, N. Mladenov, DETCHEM software package, 2.1 ed., www.detchem.com, Karlsruhe, 2006.
[19] V.V. Kislov, N.I. Islamova, A.M. Kolker, S.H. Lin, A.M. Mebel, J. Chem. Theory Comput. 1 (2005) 908.